

Rotman Lens Design and Simulation in Software

■ Christopher W. Penney

Since its invention in the early 1960s [1], the Rotman Lens has proven itself to be a useful beamformer for designers of electronically scanned arrays. Inherent in its design is a true time delay phase shift capability that is independent of frequency and removes the need for costly phase shifters to steer a beam over wide angles. The Rotman Lens has a long history in military radar, but it has also been used in communication systems.

Recently, the United States Army Research Laboratory funded a project to generate software for designing Rotman Lenses as part of an initiative to develop low-cost electronic scanning arrays for communication systems operating from C band (4–8 GHz) up to Ka Band (27.5–31 GHz) [2], [3]. The broadband performance of Rotman Lenses meets a key need of allowing the same antenna system to serve multiple functions, thus further reducing cost, complexity, and weight. The project focused on microstrip and stripline designs due to their relative simplicity of construction compared to precisely-machined waveguides.

This article uses the developed software to design and analyze a microstrip Rotman Lens for the Ku band. The initial lens design will come from a tool based on geometrical optics (GO). A second stage of analysis will be performed using a full wave finite difference time domain (FDTD) solver. The results between the first-cut design tool and the comprehensive FDTD solver will be compared, and some of

the design trades will be explored to gauge their impact on the performance of the lens.

Rotman Lenses Briefly

A Rotman Lens is a parallel plate device used to feed an antenna array. It has a carefully chosen shape and appropriate length transmission lines to produce a wave front across the output that is phased by the time delay in the signal transmission. Each input port will produce a distinct beam, shifted in angle at the output, so sweeping the beam requires feeding a different port or feeding combinations of ports. A general layout is shown in Figure 1, where the input (beam) ports are to the left and the output (array) ports are at the right. By design, there are three perfect focus beams with other beam ports surrounding them that have slightly less than perfect focus.

The design of the lens is controlled by a series of equations that set the focal points and array positions. The inputs during the design of the system can include the desired scan angle of the array, the frequency and bandwidth of the lens, the number of beams and array elements desired, and the spacing of those elements. Other factors in the design will include the fabrication technique (typically microstrip, stripline, or waveguide) and required size. The lenses can be fairly large, on the order of hundreds of square wavelengths, so high dielectric constant substrates are often used to reduce the size and, in some cases, the weight of the lens. A single lens will typically produce a fan beam, depending on the antenna array used, so several lenses can be stacked to shape the beam in a second direction.

*Christopher W. Penney (christopher.penney@remcom.com)
is with Remcom Inc., State College, Pennsylvania, USA.*

Digital Object Identifier 10.1109/MMM.2008.929774

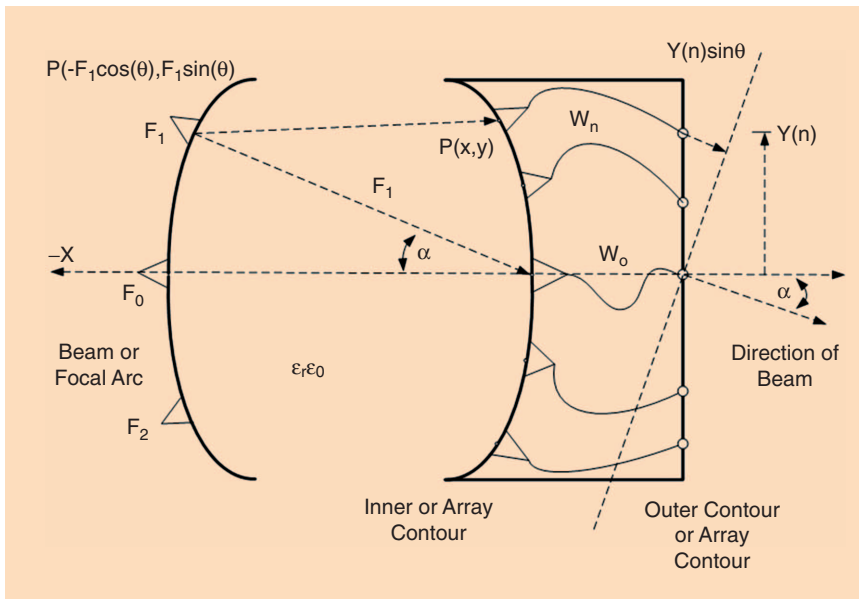


Figure 1. A basic Rotman Lens design with several of the important parameters identified. The input (Beam) ports are on the left while the output (Array) ports are on the right. Here F_0 , F_1 , and F_2 are the perfect focus points for the beams. The figure shows how inputting a signal from a beam offset by angle α will produce a wavefront with this same direction.

While the design equations are quite well known and reasonably simple to program, they do not take into consideration all of the real-world effects that may affect the performance of a lens. The full wave analysis will reveal the impact of interference from waves reflected off of sidewalls and from other ports. Interference effects will disrupt the phase front and cause irregularities in the beam shape. Another issue could be cross talk from adjacent transmission lines or reflection from the port tapers as the transmission lines transition to the parallel plate of the lens.

The Lens Design Tool Kit

The software used for the initial, theoretical design of the Rotman Lens, called Rotman Lens Designer (RLD) by Remcom Inc., is based on the equations of the lens as developed by Rotman [1] combined with GO. It is an interactive program that allows the user to enter

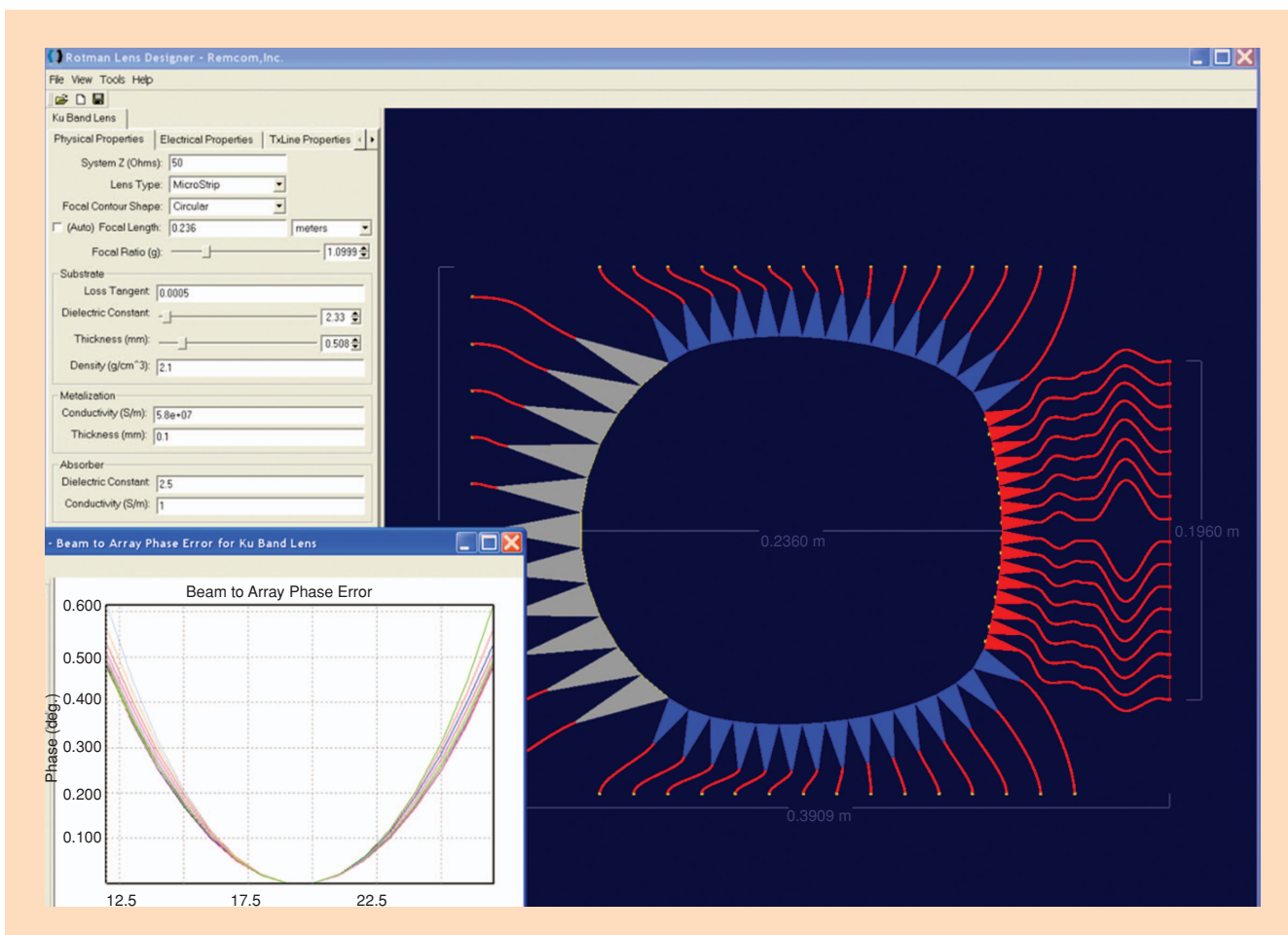


Figure 2. The Rotman Lens Designer software allows interactive adjustment of the various lens parameters while viewing the impact on the lens design and performance. Here the Ku band lens is shown with a plot of the phase error.

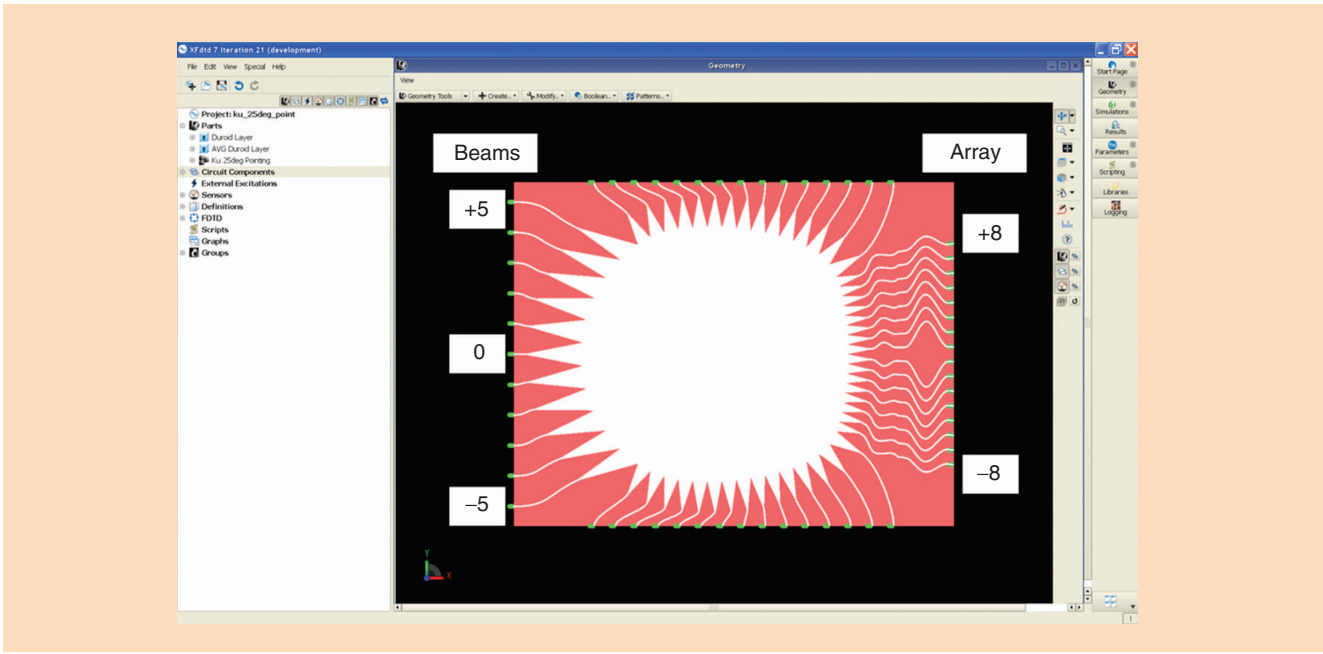


Figure 3. The initial design from RLD is imported into XFDTD as a CAD object and the project parameters are set. Here the beam and array ports are labeled for reference. The white portions of the geometry are the metal while the red portion is the dielectric substrate.

and modify a variety of parameters while viewing the impact on the lens shape and performance. Output values such as the phase error or array factor of the lens will update in real time as the parameters are adjusted, while other values such as S-parameters and insertion loss can be computed once a lens shape is set. A screen shot of the software is shown in Figure 2, where an example lens is shown along with some of the menus and an output plot. The design process implemented in the software is based in large part on that developed by Hansen [4]. The software assumes that parasitic coupling and transmission line and material dispersion are negligible while dummy load effectiveness is ideal. Effects included are the direct and singly reflected

rays propagating between ports and the impact of dielectric losses. The port voltage standing wave ratio (VSWR) is approximated as are the transmission line losses.

The full wave solver used is XFDTD v7.0 from Remcom Inc. The initial design from the RLD program may be imported into XFDTD as a computer aided design (CAD) file as shown in Figure 3. The more rigorous FDTD simulation will take into account most of the factors approximated by the simpler RLD software. An FDTD solver breaks the geometry into many small samples and updates the electric and magnetic fields on the edges of these samples as a function of time. The sample size must be one-tenth of a wavelength or less, so for geometries of many hundreds of square

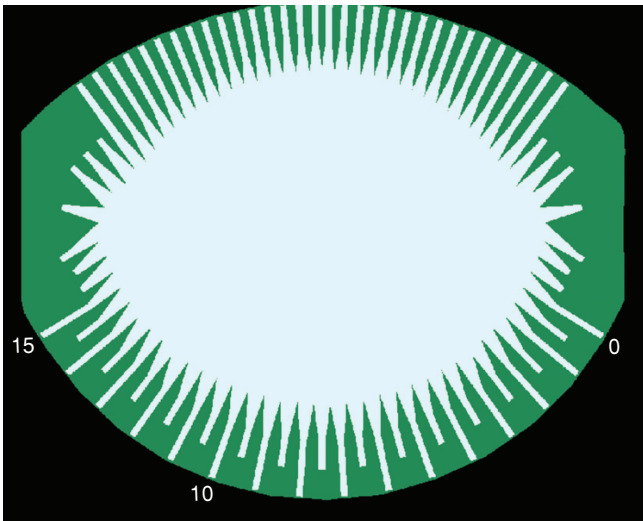


Figure 4. Shown is the geometry of an X-band Rotman Lens simulated with XFDTD and compared to measured results. The results were previously published in [5].

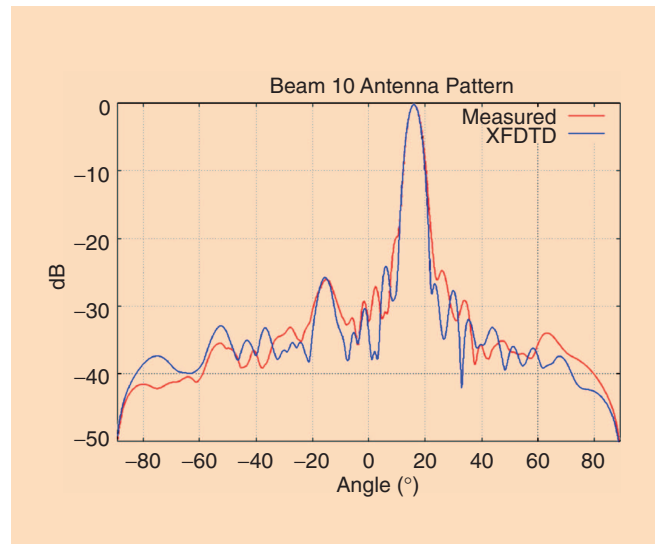


Figure 5. The array factor for the Rotman Lens of Figure 4 comparing simulated XFDTD results to measurements.

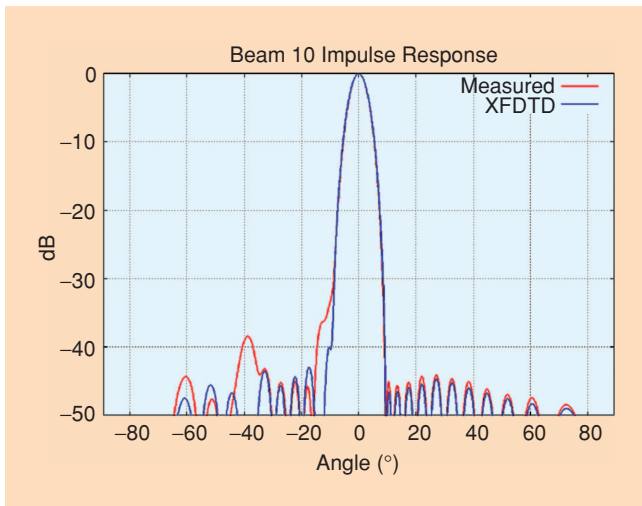


Figure 6. The impulse response of the Rotman Lens in Figure 4 comparing simulated XFDTD results to measurements.

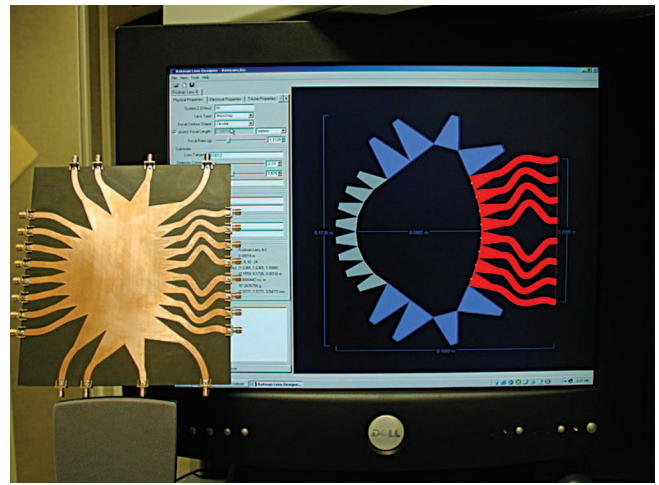


Figure 7. Shown is a 10-GHz Rotman Lens designed using the RLD software and fabricated (photo courtesy of Dr. Erik Lenzing).

wavelengths, the computer resources needed are fairly significant. However, these problems are well within reach of current desktop personal computers (PCs).

Previously, the XFDTD software was used to simulate Rotman Lenses with very good agreement with measurements [5]. In that case, an existing X-band lens was simulated to validate the simulation results for S-parameters

and beam patterns against measured results. The XFDTD model of the lens is shown in Figure 4, while some simulated beam patterns compared to measurements are shown in Figures 5 and 6.

The intended design process should start with the definition of the desired performance of the lens, then the RLD tool should be used to develop a rough design. The initial

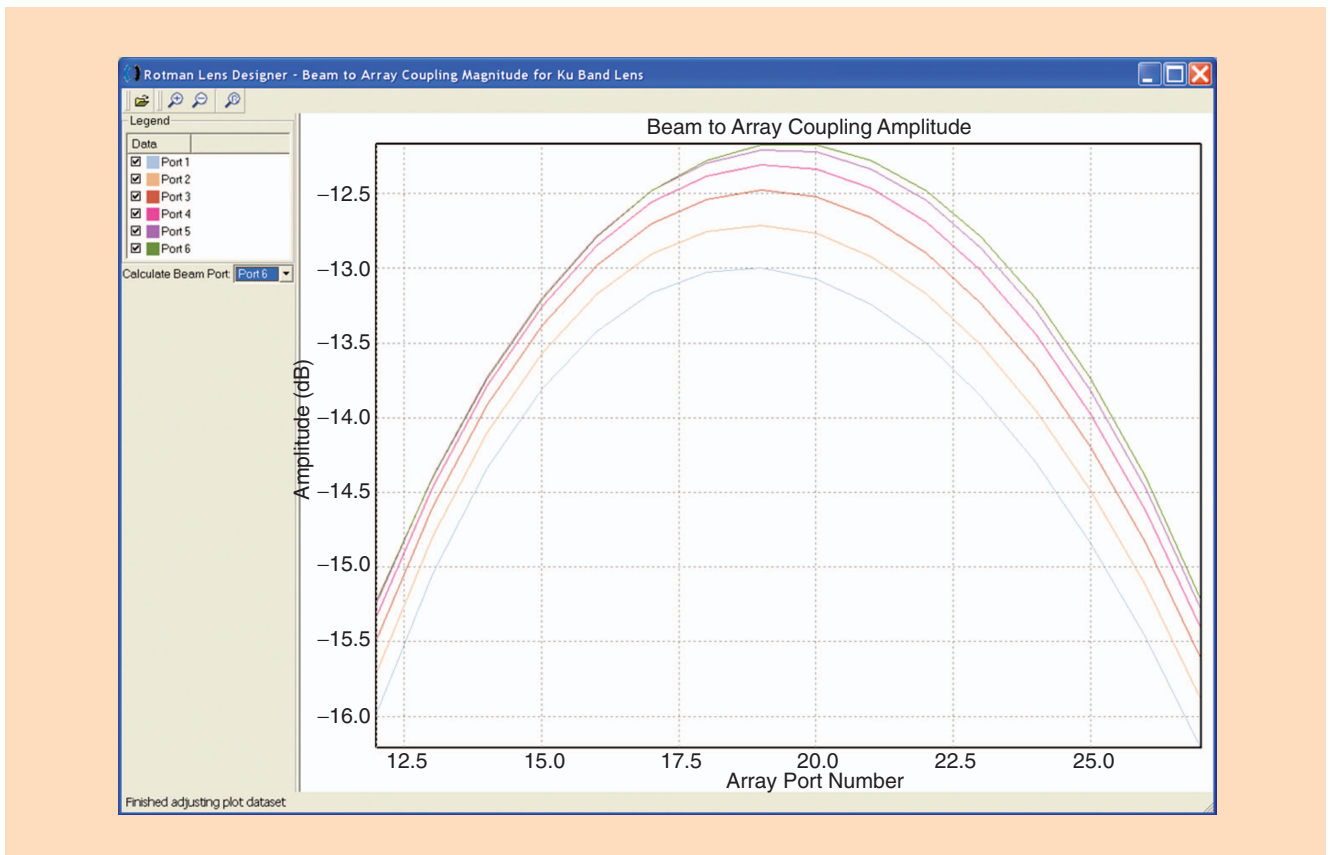


Figure 8. The amplitude distribution of the lens across the array ports from each beam has a roll off of about 3 dB. Here the beam to array coupling amplitude computed by RLD is shown.

Since its invention in the early 1960s, the Rotman Lens has proven itself to be a useful beamformer for designers of electronically scanned arrays.

design can be tuned for best theoretical performance within RLD, and then the design can be exported for fabrication or further analysis. The full wave XFDTD solver may then be used to verify the RLD results and perform fine tuning, as needed on the design. On its own, the RLD designer has been used to develop a C-band lens for the U.S. Army that was fabricated. The measured results for the lens showed good agreement with those from the GO-based RLD software [3]. Also, an X-band lens with a center frequency of 10 GHz was designed using RLD, and good results with full wave simulations and measurements were found [6]. Figure 7 shows both the RLD model of the X-band lens on screen and an actual fabricated lens constructed from the RLD model.

An Example Lens Design

Geometrical Optics Solver

To demonstrate the software, a realistic example lens will be designed and simulated. The design parameters are based on those used previously by the Army Research Lab [2]. The lens will have eleven beams and a scan angle of $\pm 25^\circ$ at a center frequency of 16 GHz with a 4 GHz bandwidth. There will be 16 array ports suitable for a 16-element antenna array, and the element spacing will be 13 mm or about 0.7 wavelengths.

With the above design parameters, some choices can be made for the other parameters of the lens. We will choose to make the lens as a microstrip with a 50Ω impedance transmission lines and a Duroid substrate of 0.5 mm thickness and a dielectric value of 2.33. The lens will have a circular curvature on the beam port side and moderately rounded sidewalls ending in a number of dummy ports to absorb energy and reduce reflections. To obtain better performance, the beam and array ports will be adjusted so that each tapered line is pointing toward the center of the lens on the opposite side rather than being normal to the lens surface. This is

described as *port pointing* and improves the response of the outer beams, as we will show later. As for the size and focal length of the lens, the width will be fixed at 236 mm, or about 19.5 wavelengths. This size is chosen to match the width of the lens constructed in [2].

Once the main parameters are set, a lens is created that will require tuning to obtain the desired performance. Typically, the tuning involves viewing an output quantity such as the phase error across the array port or the array factor (beam pattern) while adjusting the focal ratio of the lens. The focal ratio is a factor that is related the curvature of the lens and, as the name implies, focuses the lens. A poorly focused lens will produce a messy beam pattern, while a properly focused lens will yield a distinct beam. For the array factor, a set of symmetrical beams, shifted in angle, with low side lobes is desired. A final design with well-focused beams was reached with a focal ratio of 1.099.

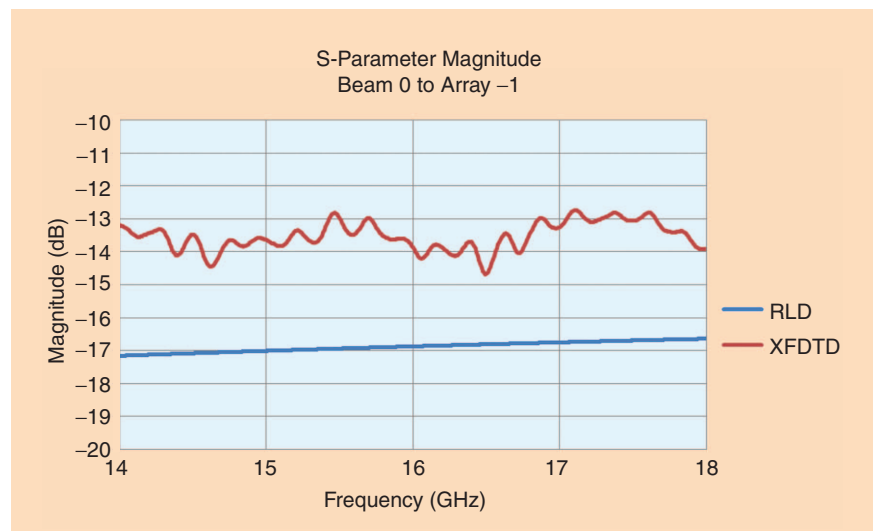


Figure 9. Plotted is the S-parameter magnitude over the frequency range of the lens at array port -1 with beam 0 active.

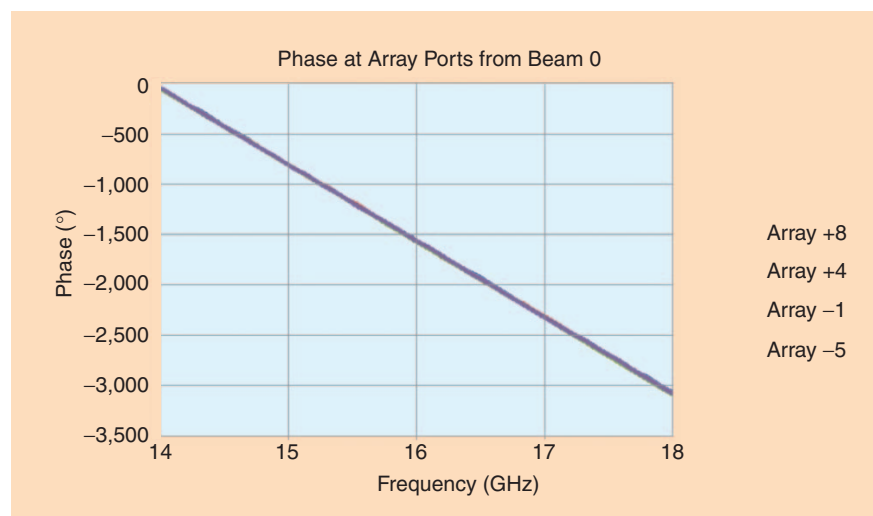


Figure 10. The phase generated by the full wave FDTD solver at the array ports is linear over the entire frequency range of the lens.

Forming good beams also produces low phase error across the array ports, and for this lens, the error is less than one degree for every port. The lens is designed with an amplitude distribution that rolls off about 3 dB from the center of the array ports to the edges, as shown in Figure 8. Each plot shows the distribution across the output from one of the beam ports.

The sidewall curvature is arbitrarily set at a unitless value of 0.75, which produces a slightly curved edge. Since the dummy ports are assumed to be ideal, there will be little change in the output plots generated by RLD between different sidewall curvature settings. The impact of the sidewall curvature will have to be examined in more detail by the full wave solver. The aperture width of the dummy ports is chosen to be about the same as that of the beam ports, giving 16 dummy ports per sidewall. Again, the impact of the sides and number of dummy ports will need to be examined with the full wave solver later.

One other interesting parameter that can be varied is the taper angle of the ports, which transition the transmission

While the design equations are quite well known and reasonably simple to program, they do not take into consideration all of the real-world effects that may affect the performance of a lens.

lines to the lens. The angle of this taper region will affect the VSWR of the ports. A default setting of 11° is chosen for the initial design, and later, the impact of this parameter will be examined using the full wave solver.

Transmission lines are added to all ports with the most critical ones being those attached to the array ports. The relative lengths of these lines are set by the design equations, and any error in those lengths will throw off the phasing. However, a fixed length of line may be added to each and is typically needed to be able to route the lines as needed to the antenna array while maintaining good separation distances between the lines. The RLD software will construct the lines but does not include any effects of crosstalk between lines. So, some care must be used to avoid getting the lines very close together and simulation with the full wave solver will be needed to ensure there are no issues related to the lines.

Once the final design is reached, the lens can be exported as a CAD file for use in fabrication or for loading into another solver. In this case, the lens will be sent to the FDTD solver for further analysis.

Full Wave Solver

The metal portion of the lens design is typically imported as a CAD file into the FDTD software. The dielectric substrate and the ports at the ends of each line must be added. As the lines are designed with $50\ \Omega$ impedance, the ports will each contain a voltage source with $50\ \Omega$ source impedance as well. For the S-parameter analysis, one beam port at a time will be chosen as active. The input signal to the active port is a broadband Gaussian pulse, which will excite frequencies over the entire bandwidth of the lens. The results collected will be time-domain signals of voltage and current at each port, which are then transformed to the frequency domain to give S-parameters, impedance, and other output quantities.

A critical step in the FDTD analysis is the creation of the FDTD mesh. In

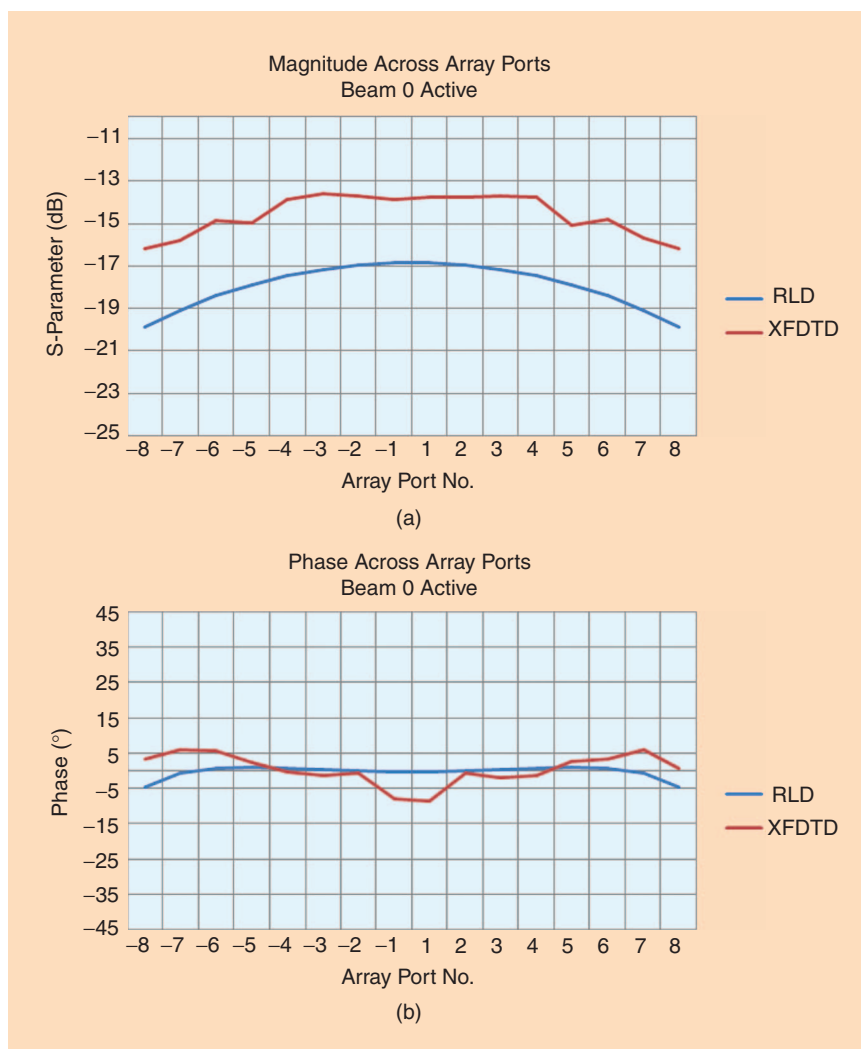


Figure 11. (a) The S-parameter magnitude across the array ports at the center frequency of the lens shows a 3 dB taper from the center to the edges. (b) The phase across the array ports is close to linear. The plots are at the center frequency of 16 GHz.

In addition to constant magnitude response versus frequency, it is desirable to have linear phase response with frequency as well.

general, good results require that each transmission line is several cells across to give accurate sampling of the fields. A recent advancement added to the XFDTD solver is a feature that locates the edges of all geometry objects and adjusts the mesh size local to that object to ensure that the object's edges are clearly defined by an FDTD cell edge. This feature is known as fixed-point extraction, and it creates a precise mesh with nonuniform cell dimensions with minimal user intervention. The benefit of this approach is that it can save significant amounts of computer memory for most structures and greatly simplifies the meshing process for the user. For the example lens created here, the mesh contains about 45 million cells with a maximum cell size of 0.5 mm and a minimum cell size of 0.1 mm. The calculation requires about 1.4 GB of memory to solve. While these calculations would fit on a standard 32-b desktop PC, we will run the simulations using a much faster hardware minicluster, where a pair of NVIDIA FX 5600 GPU cards has been specially programmed to simulate the FDTD equations. The simulations typically require 40,000–60,000 steps in time to reach convergence, and execution times on the hardware cluster are typically between one and one-half and two hours. As the geometry structures are symmetrical about the centerline, it would have been possible to cut the geometry in half and mirror it using an appropriate boundary condition. This approach would save a significant amount of memory and cut the simulation time, but given the speed of the hardware platform, the setup time for the user to create the mirrored geometry would have negated the simulation time savings. If the geometry structure of the Rotman Lens were so large that the FDTD mesh would not fit in memory, this mirroring approach becomes essential to run the calculation.

Results

After finishing the lens design and setting up and running a few simulations for several different beams, we can begin to compare results between the GO solver and the full wave solver. We are

interested in several output quantities, including the S-parameters at the array ports and the beam patterns generated by the array. We will compare the S-parameter magnitude and phase, both as a function of frequency and as a function of array port, to ensure that the response matches our design goals.

The most basic data that can be compared between the two programs is the array port S-parameters. Each array port will have transmission S-parameter from each beam port that varies as a function of frequency. In Figure 9, we can see that the S-parameter magnitude results from the GO solver for the center beam are linear and nearly constant with frequency. The full wave solver results are based on the voltage and current values received at the array port. They are clearly more complex but still fairly constant across the frequency range showing good transmission for any frequency. There is an offset in the results where the GO results are several dB lower than the full wave solution caused by the worst-case

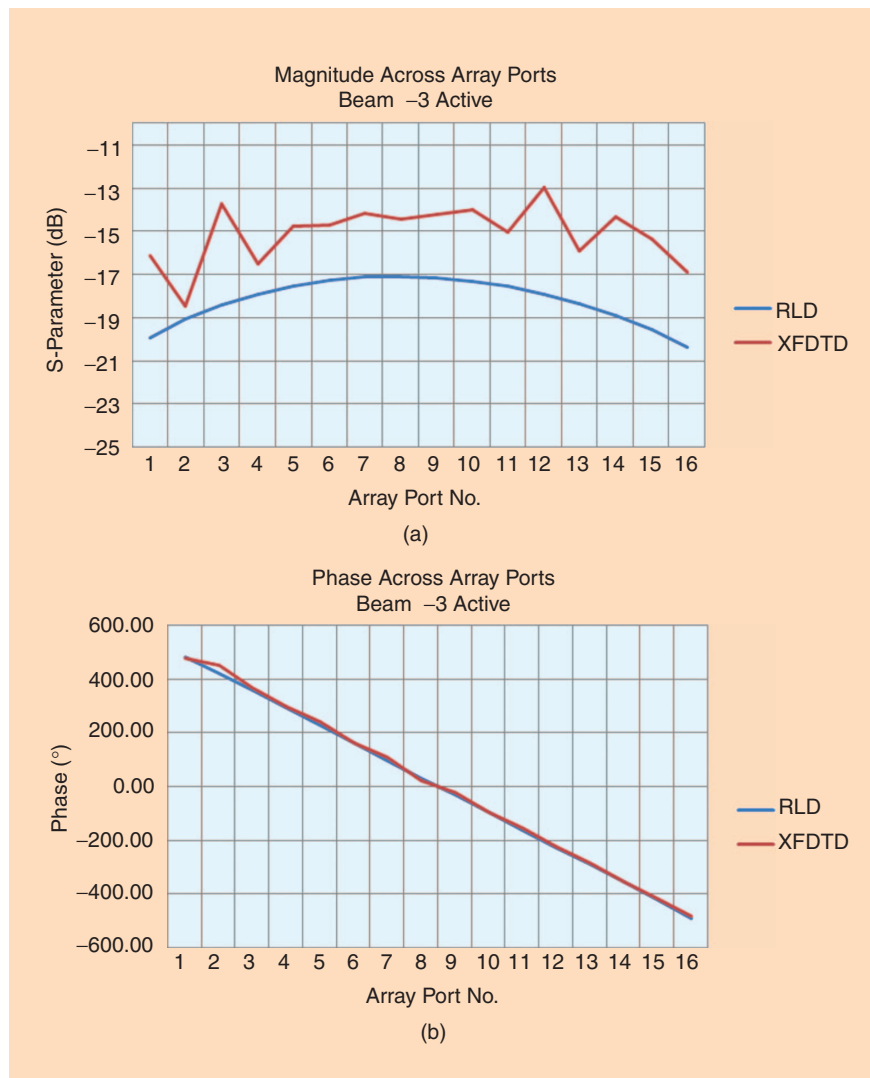


Figure 12. (a) For beam -3 active the magnitude across the array ports (top) shows some variation in the full wave solution that is not present in the geometrical optics solution. In part the variations could be from sidewall reflections. (b) The phase shift across the array ports is very close to linear.

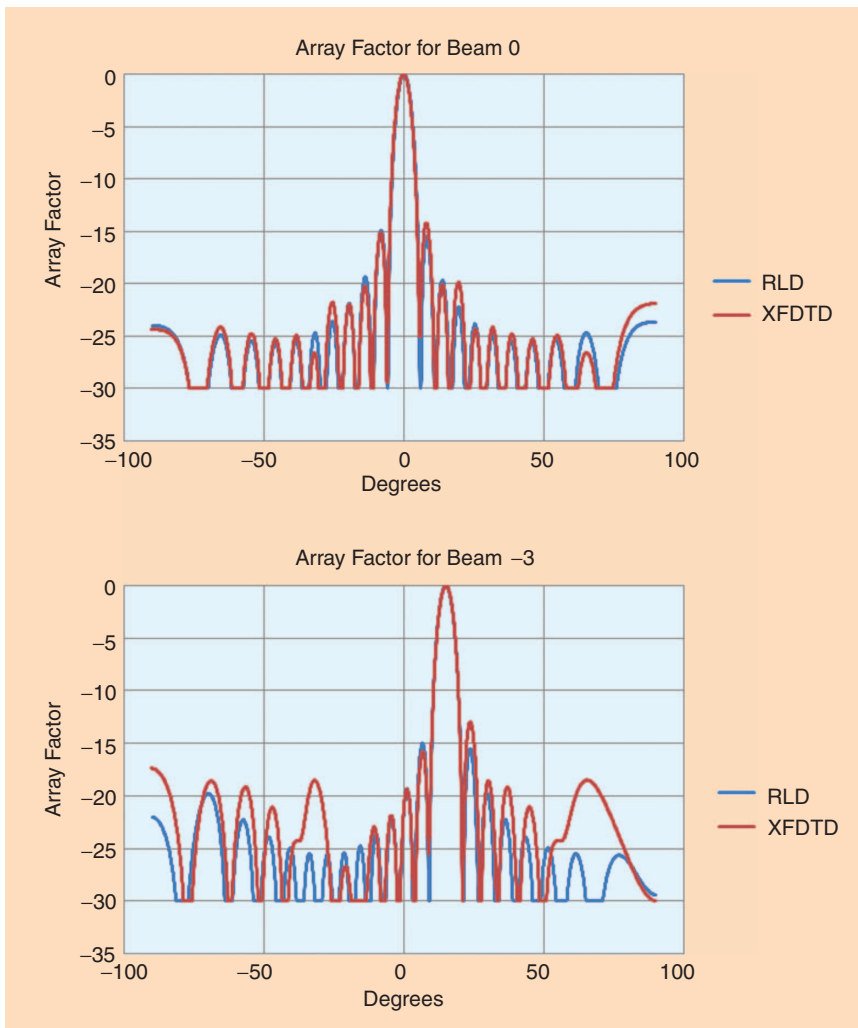


Figure 13. The array factor for the lens shows a strong central beam and very close agreement is found between the geometrical optics and full wave solutions. The top plot is for the center beam while the lower plot is for one of the offset beams.

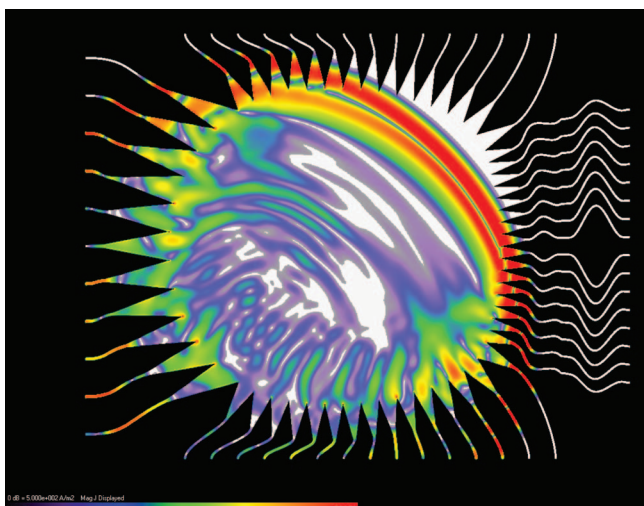


Figure 14. The current propagating across the lens from the -5 port (lowest left) shows the wave front will hit many of the dummy ports with similar amplitude levels as the array ports.

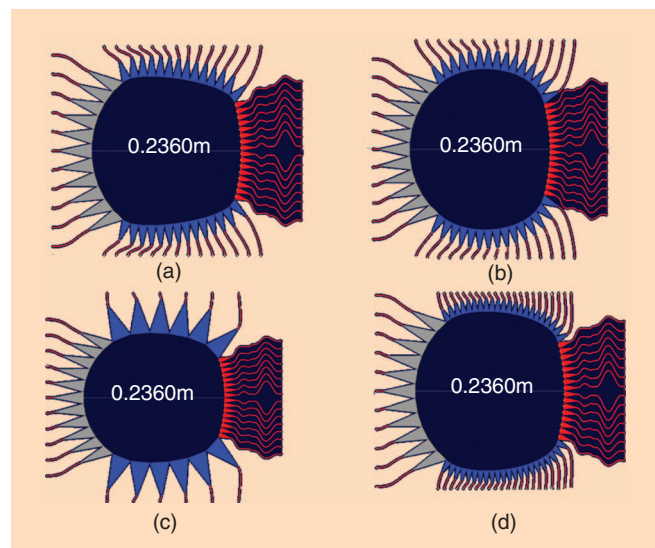


Figure 15. Several variations were made to the lens sidewalls, including (a) and (b) decreasing and increasing the curvature and (c) and (d) changing the size and number of dummy ports.

assumptions made in the RLD software about the losses in the lens. Results for other beam and array combinations are similar.

In addition to constant magnitude response versus frequency, it is desirable to have linear phase response with frequency as well. In Figure 10, the phase of the S-parameter is plotted and we can see that for several array ports, the phase shift as a function of frequency from the full wave solver is quite linear. Note that the phase response was unrolled to give a linear plot rather than a saw-tooth pattern that would come out by default. The results for other beam and array ports and from the GO solver are similar.

After comparing the frequency response, we can look at the results at the designed center frequency of the lens as a function of array port. These results are obtained by extracting the magnitude and phase data at the center frequency from the frequency-domain S-parameter data generated by the software. This process is handled by user-generated scripts that are supported within the software for data processing.

First, the center frequency S-parameter magnitude across the array ports for beam 0 (center port) active are compared. Our design called for a 3 dB roll-off of the magnitude toward the ends of the array, and this does appear to be the

case as shown in Figure 11(a). Again the GO results are lower due to higher losses assumed, but the shape of the plots shows decent roll-off. For beam 0, the phase response [Figure 11(b)] should be flat across the array ports since each is about the same distance from the center beam port. The results indicate this within about $\pm 5^\circ$ of variation. Similarly, for beam -3 (see Figure 3 for beam locations), the magnitude response across the array ports shows the desired roll-off, although in the full wave results, there are some discontinuities in the curve at the outer array ports (see Figure 12). The phase response for beam -3 is quite linear across the array and there is high correlation between the GO and full wave results.

During the design process, the shape of the array factor was used to tune the lens. The array factor is computed as the pattern that would be generated by a linear array of elements at the output port locations. The factor is extracted from the full wave solver data by taking the Fourier transform of the time-domain port voltage at each output port location and using the complex frequency-domain voltages as the sources for the linear array. Again, this postprocessing is handled by a user-generated script in the software, and the magnitudes are normalized to the peak value. For beam 0, the array factor comparison between the GO and full wave solvers are nearly identical, with only slight variations in the side lobe levels. For beam -3, the array factor results have more variation in the side lobes, but the main beam and major side lobes show very good agreement. The array factor plots for the two beams are shown in Figure 13.

Based on these results, it appears the GO solver is providing a very good design for the lens as the agreement with the full wave solver is close. However, since the GO solver makes a number of simplifying assumptions, it might be interesting to try some variations of the lens design to see the impact on the results as compared to the full wave solution. One seemingly major simplification is that only direct and singly reflected rays are included in the GO solution, and absorption by

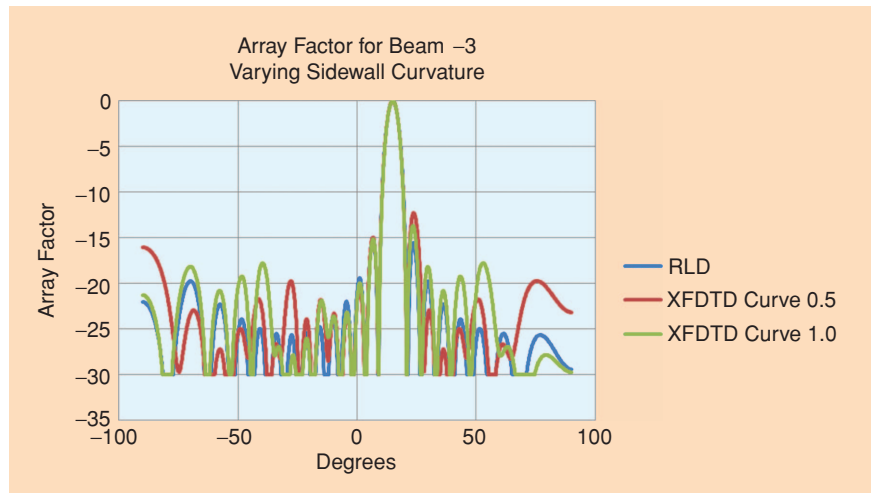


Figure 16. When the sidewall curvature is changed, the side lobe levels and positions shift, indicating that small reflections from the sidewalls are interfering with the signal received at the array ports. However, the main beams are very similar between all cases.

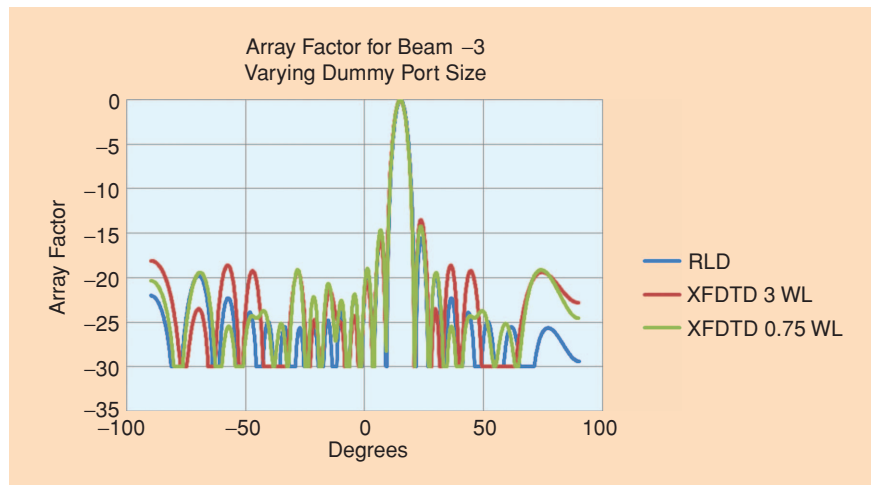


Figure 17. Changing the size of the dummy ports on the sidewalls has a smaller impact on the array factor.

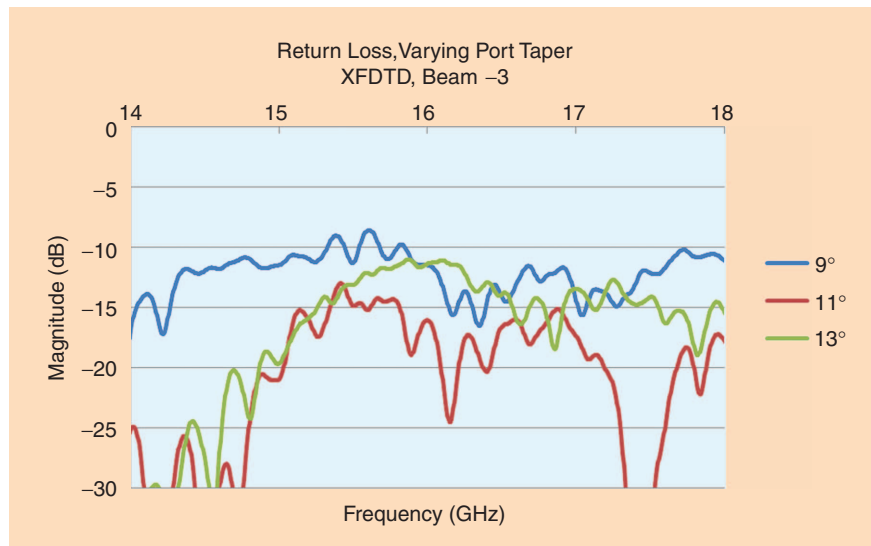


Figure 18. The return loss over the frequency range of the lens shows that 11° and 13° tapers give better results than the longer nine degree taper.

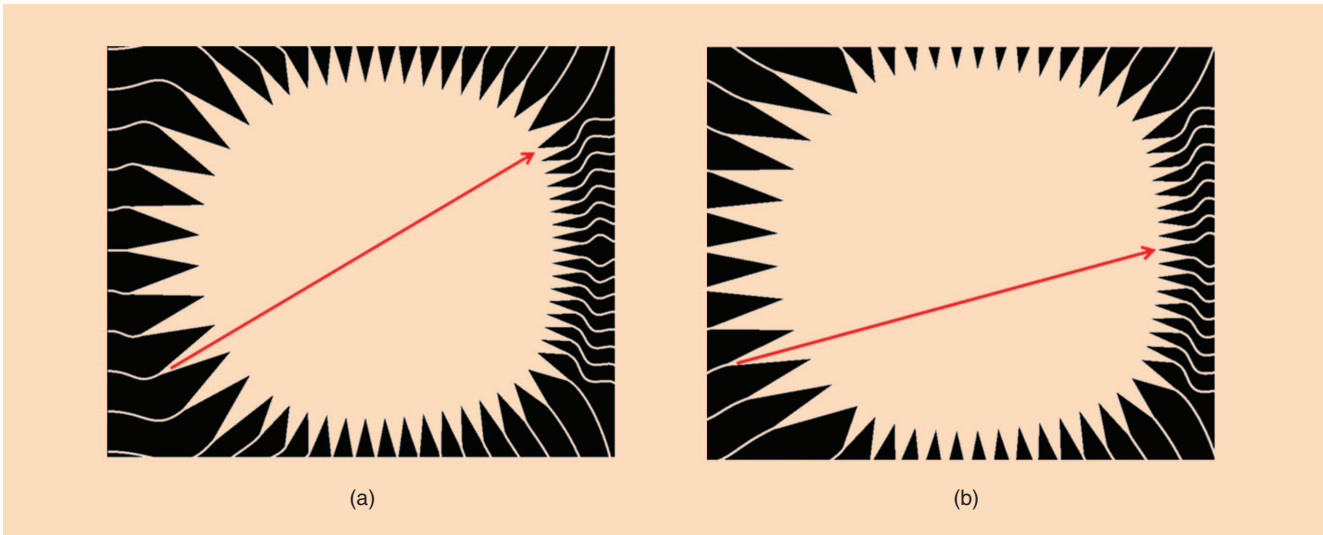


Figure 19. (a) The lens has ports that are attached normal to the lens curve. This can result in beam ports that point toward the sidewalls of the lens. (b) By turning on port pointing in the RLD software, each port is tilted so it is focused toward the center of the opposite side of the lens.

the dummy ports is considered to be ideal. In our previous results, the center beam agreement was much better between codes than the offset (beam -3) port. Certainly, the radiation from the lower beams will have much greater interaction with the sidewalls than the center beam. To show this more clearly, the propagation of current on the lens surface from the lowest beam port (beam -5) is shown in Figure 14, and it is clear that a good portion of the high amplitude signal will hit the sidewall and go into the dummy terminals.

To gain a better perspective on the design choices, we will vary both the curvature of the sidewalls and the size and number of dummy ports in our original lens design and compare results. First, the sidewall curvature will be increased and decreased while keeping the dummy port aperture size fixed, as shown in Figure 15(a) and (b). This

causes the flatter sidewall case to lose one dummy port. To test the impact of dummy port size, the sidewall curvature will remain the same while the dummy port aperture size is varied, as shown in Figure 15(c) and (d). The original dummy port apertures were sized at 1.1 wavelengths in width, giving 15 ports on each sidewall. We'll now increase the port size to 3 wavelengths to drop the number per sidewall to six and decrease the port size to 0.75 wavelengths to increase the number of ports per sidewall to 22. The GO results for all cases are virtually the same as the original design since the sidewall changes have little impact on the equations used in that solver. The full wave results show that the variations in the lens sidewall curvature shift the levels in the minor side lobes (Figure 16) that are down more than 15 dB from the main beam. However, the main beam shape and position remain constant, so the

fields reflected from the sidewalls are fairly weak. Similarly, changing the dummy port sizes has some impact on the side lobe levels, but no visible impact on the main beam (Figure 17). Changing the dummy port sizes had very little impact on the magnitude of the signal reaching the array ports for any of the beams simulated. This indicates that the sidewalls are not contributing strong reflections that are disturbing beam patterns and little energy is lost to the dummy ports.

Another simplifying assumption of the GO solver relates to the calculation of losses and VSWR in the ports. The most relevant characteristic of the design that relates to the port VSWR is the shape of the transition region between the transmission lines and the

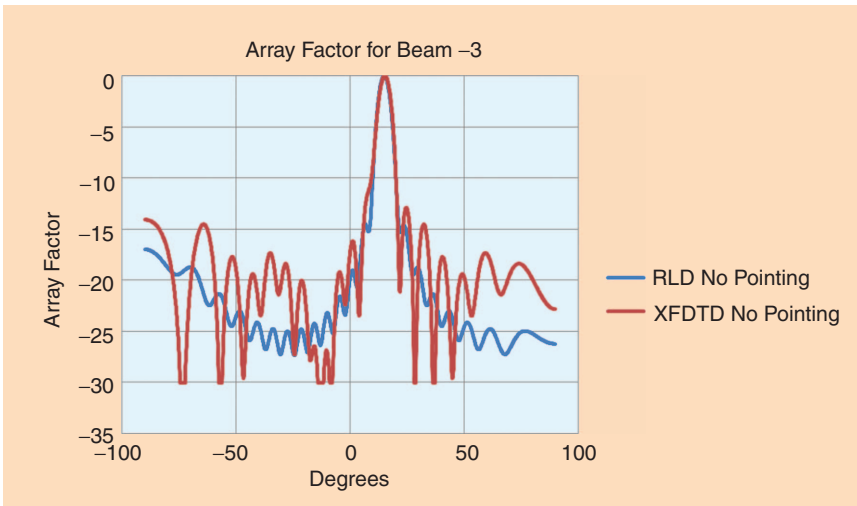


Figure 20. With no port pointing used, the array factor for beam -3 degrades resulting in a poorly defined main beam with higher side lobes. In contrast, the lens with pointed ports has a smoother beam (shown in Figure 13).

lens. This shape is controlled by the port taper adjustment in the GO solver, which specifies an angle for the taper. The default design used a taper angle of 11° , which gives a port length of about 50 mm. We will adjust the port taper angle up and down to 13° and 9° , which gives taper lengths of 40 and 60 mm, respectively. Here we will look at the return loss from the ports as a function of frequency since that is the factor that will be most affected by the change. The GO solver gives a constant return loss of about -12 dB for all the ports across the entire frequency range. When the full wave results are computed, they show significant variation in the return loss (Figure 18). Although all results are acceptable, it appears the 11° and 13° taper angles give better return loss (lower reflection) across the frequency range than the 9° taper.

As a final investigation, let's look into the matter of port pointing. With no port pointing, the beam and array ports are attached normally to the lens surface. In some cases, this can result in the outer beam ports pointing more toward the sidewalls than toward the array ports. It has become customary to attach the ports so they are pointed toward the center of the opposite side of the lens. Examples of each configuration are shown in Figure 19. It makes sense that having the ports pointed toward the desired location will result in better lens performance, and this is easy to see in Figure 20, where the array factor for beam -3 is plotted with no pointing. Previously, with port pointing applied (Figure 13), this beam showed a clean array factor with a well formed beam. Now with pointing turned off, the array factor is nonsymmetrical with higher side lobes. The agreement between the GO and full wave solvers is much lower here too as the fields propagated by the beam port will have much more interaction with the sidewall and dummy ports. This is a good indication that using pointing will result in better lens performance and reduced losses to the sidewalls.

A further question to ask related to pointing is whether pointing the port toward the center of the opposite side of the lens will give the best performance for every situation. To experiment with this, the port angle for beam -3 with respect to the default pointing direction is parameterized in the full wave solver (Figure 21), and the resulting array factors for each case are compared. The middle position in Figure 21 is the pointing position and rotations of $\pm 5^\circ$ and 10° are applied to the port. Following the simulation, the results show that increasing the pointing angle by 5° for this beam in this lens did give a very slightly more symmetrical beam pattern with lower side lobes. While the improvement is small in this example, it could be that for another lens, a more significant improvement might be possible. However, the overall conclu-

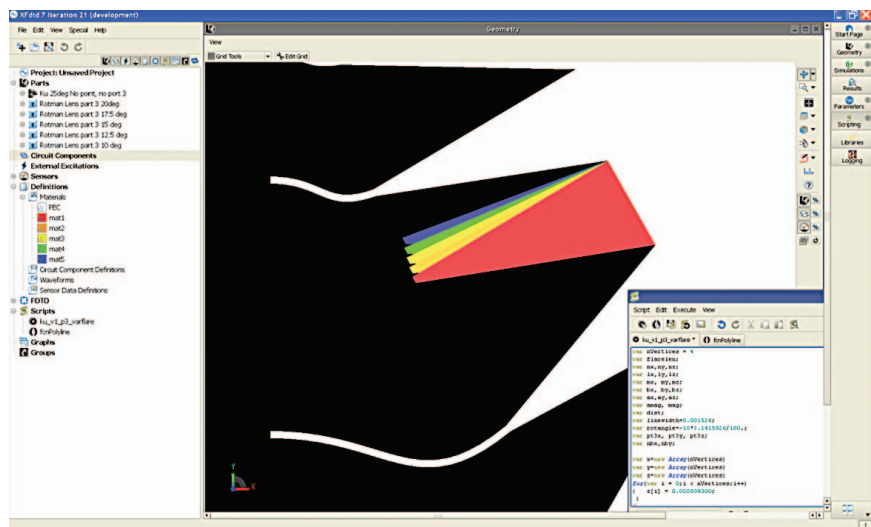


Figure 21. Several shifted variations for the port at beam -3 are shown to demonstrate the range of values simulated. When performing the simulations, only one port at a time was connected with the associated transmission line.

sion is that the default pointing works quite well and is certainly preferred over nonpointing ports.

Conclusion

In this article, two software tools for the design and simulation of Rotman Lenses were compared using a realistic example of a Ku-Band lens. The performance of the simpler, GO tool was found to be quite good compared to the more rigorous full wave solution. While the GO tool makes a number of simplifying assumptions, the results from several parameter sweeps indicate that those assumptions are valid. For the example studied here, the main area where the GO assumptions affect the results, the reflections from the sidewalls, did not significantly alter the beam patterns generated by the lens. In other lens designs, the impact of the simplifying assumptions of the GO solver may be greater, so validation with the full wave solver is certainly recommended. Overall, the two products provide a simple means to generate and fully analyze these complex devices.

References

- [1] W. Rotman and R. Turner, "Wide-angle microwave lens for line source applications," *IEEE Trans. Antennas Propagat.*, vol. 11, no. 6, pp. 623–632, Nov. 1963.
- [2] O. Kilic and S. Weiss, "Dielectric Rotman Lens design for multi-function RF antenna applications," in *Proc. 2004 IEEE AP-S Int. Symp.*, June 2004, vol. 1, pp. 659–662.
- [3] S. Weiss, S. Keller, and C. Ly, "Development of simple affordable beamformers for army platforms," presented at 2007 GOMACTech Conf., Lake Buena Vista, FL, Mar. 2007.
- [4] R.C. Hansen, "Design trades for Rotman Lenses," *IEEE Trans. Antennas Propagat.*, vol. 39, no. 4, pp. 464–472, Apr. 1991.
- [5] C.W. Penney, R.J. Luebbers, and E. Lenzing, "Broad band Rotman Lens simulations in FDTD," in *Proc. 2005 IEEE AP-S Int. Symp.*, July 2005, vol. 2B, pp. 51–54.
- [6] S. Albarano III, E.H. Lenzing, C.W. Penney, and R.J. Luebbers, "Combined analytical-FDTD approach to Rotman Lens design," presented at the 22th Annual Review of Progress in Applied Computational Electromagnetics, Miami, FL, Mar. 2006.